Check for updates

Received: 7 July 2022 | Revised: 29 August 2022 | Accepted: 4 September 2022

DOI: 10.1002/jcc.27009

RESEARCH ARTICLE

Journal of COMPUTATIONAL CHEMISTRY WILEY

Solvent effects in four-component relativistic electronic structure theory based on the reference interaction-site model

Kodai Kanemaru[1] | Yoshihiro Watanabe[1] | Norio Yoshida[1,2] | Haruyuki Nakano[1]

[1]Department of Chemistry, Graduate School of Science, Kyushu University, Fukuoka, Japan

[2]Department of Complex Systems Science, Graduate School of Informatics, Nagoya University, Nagoya, Japan

Correspondence
Norio Yoshida and Haruyuki Nakano, Department of Chemistry, Graduate School of Science, Kyushu University, 744 Motooka, Nishi-ku, Fukuoka 819-0395, Japan.
Email: noriwo@nagoya-u.jp and nakano@chem.kyushu-univ.jp

Funding information
Japan Society for the Promotion of Science, Grant/Award Numbers: 19H02677, 21K04980, 22H05089

Abstract

A combined method of the Dirac–Hartree–Fock (DHF) method and the reference interaction-site model (RISM) theory is reported; this is the initial implementation of the coupling of the four-component relativistic electronic structure theory and an integral equation theory of molecular liquids. In the method, the DHF and RISM equations are solved self-consistently, and therefore the electronic structure of the solute, including relativistic effects, and the solvation structure are determined simultaneously. The formulation is constructed based on the variational principle with respect to the Helmholtz energy, and analytic free energy gradients are also derived using the variational property. The method is applied to the iodine ion (I^-), methyl iodide (CH_3I), and hydrogen chalcogenide (H_2X, where X = O–Po) in aqueous solutions, and the electronic structures of the solutes, as well as the solvation free energies and their component analysis, solvent distributions, and solute–solvent interactions, are discussed.

KEYWORDS
Dirac–Hartree–Fock, four-component relativistic method, reference interaction site model self-consistent-field, relativistic effect, solvent effect

1 | INTRODUCTION

The relativistic molecular orbital theory is now one of the essential pieces in quantum chemical theory. Currently, it is well recognized that the relativistic effects have an important role in the electronic structure of molecules containing heavy elements. In particular, the scalar and spin–orbit effect, which are classes of relativistic effects, affect the geometries, properties, and reactions of molecules through their effects on the shape of molecular orbitals and splitting of energy levels. Such relativistic effects are most naturally taken into account via the Dirac equation, which is the basic equation of relativistic quantum mechanics.[1] The Dirac equation gives four-component spinors as solutions describing the electrons and their anti-particles, the positrons. The methods based on the Dirac equation are called four-component methods, and are now widely used in quantum chemistry, along with the two-component methods. Nowadays, the relativistic Hartree–Fock (HF),[2–5] the density functional theory (DFT),[6,7] Møller–Preset perturbation,[8–10] configuration interaction (CI),[11,12] and coupled-cluster (CC)[13] methods have been developed and standardly used. In addition to the HF, DFT, and HF-based single reference methods, multiconfiguration methods, such as the multiconfiguration self-consistent field (MCSCF) method,[14,15] multireference (MR) CI,[16] MR perturbation,[17–19] and MR CC[20] methods, were developed and are being used. Recently, the four-component full CI Monte Carlo[21] and density matrix renormalization group[22] were formulated.

When considering chemical reactions in solution of molecules containing heavy atoms, solvent effects must be considered simultaneously with relativistic effects. The methods for incorporating the solvent effects on the four-component relativistic methods have been fairly limited to date, and a methods combined with the polarizable continuum model (PCM) has recently been proposed by Di Remigio

 © 2022 Wiley Periodicals LLC.

1096987x, 2023, 1, Downloaded from https://onlinelibrary.wiley.com/doi/10.1002/jcc.27009 by Kyushu University, Wiley Online Library on [21/11/2022]. See the Terms and Conditions (https://onlinelibrary.wiley.com/terms-and-conditions) on Wiley Online Library for rules of use; OA articles are governed by the applicable Creative Commons License

et al.[23] They formulated a four-component relativistic self-consistent field (SCF) theory for a molecular solute described with the PCM for solvation. In their study, the four-component Dirac–Hartree–Fock and Kohn–Sham DFT methods were combined with the integral equation formalism (IEF) PCM[24] to successfully determine the electronic structure of the solute and the continuum model of the solvent in a self-consistent manner. After being proposed, this method has been applied to the calculations of electron paramagnetic resonance and nuclear magnetic resonance (NMR) parameters, and so forth.[25] The four-component relativistic polarizable embedding was also presented by Hedegård et al. in 2017.[26]

In the present article, we present the four-component Dirac–Hartree–Fock reference interaction-site model self-consistent field (DHF/RISM-SCF) method, which combines the relativistic four-component method with the reference interaction-site model (RISM), and its geometrical derivative have been formulated and implemented. RISM[27,28] is a statistical-mechanical integral equation theory for molecular liquids, which is derived from the functional derivative of the grand potential for solute–solvent molecular pair interactions with respect to the density function. Features different from the PCM are that the RISM theory can account for intermolecular interactions such as hydrogen bond and that it can provide a solvation structure around the solute molecule. Furthermore, an analytical solvation free energy expression is known and can be evaluated based on a first-principles approach. These advantages have led to its use in the analysis of various chemical processes in solution.[28] A hybrid method of quantum chemical electronic structure and the RISM theories, called RISM-SCF method, was proposed by Ten-no et al. in 1993.[29,30] The coupled equations of the Hartree–Fock and RISM equations derived by them are solved self-consistently, and the electronic wave function of the solute molecule and the solvent distribution can be determined simultaneously. Following their study, the combination of the theories has been variously extended both in the electronic structure and integral equation theories.[31,32] Therefore, the RISM theory is also effective in introducing solvent effects into the relativistic electronic structure theory. The DHF/RISM-SCF method presented here, enables the simultaneous description of the detailed solute electronic structure based on the relativistic electronic structure theory and the solvation structure based on molecular theory.

The present article is structured as follows: The DHF/RISM-SCF method based on variational formalism as well as its analytical energy gradient method is presented in Section 2; the computational details are given in Section 3; the applications to several systems (the iodine ion I^-, methyl iodide CH_3I, and hydrogen chalcogenides H_2X (O–Po)) are discussed in Section 4; and conclusions are drawn in Section 5.

2 | METHOD

The RISM-SCF method is formulated as a variational problem for free energy, which was initially proposed by Sato et al.[31] for an MCSCF wave function. Here, we consider a system in which a quantum mechanical solute molecule is immersed in a solvent composed of classical molecules at infinite dilution. In this formulation, the basic equations are derived from the stationary conditions for the Helmholtz energy Lagrangian:

$$L(\mathbf{C},\boldsymbol{\zeta}^{\mathrm{U}},c,h,t)=E^{\mathrm{U}}(\mathbf{C})+\Delta\mu(\mathbf{C},c,h,t)+\boldsymbol{\zeta}^{\mathrm{U}}\times\boldsymbol{e}^{\mathrm{U}}(\mathbf{C}). \tag{1}$$

The first term of the right-hand side in Equation (1) represents the electronic energy of the solute molecule and $\mathbf{C}$ is the set of the variational parameters in the wave function. The second term represents the excess chemical potential of solvation, and c, h, and t are the direct, total, and indirect correlation functions describing the solvent structure around the solute molecule, respectively. The third term corresponds to constrains on the parameters ($\mathbf{C}$) in the solute wave function; that is, the orthonormality of orbitals and/or the normalization of the wave function. The symbols $\boldsymbol{e}^{\mathrm{U}}$ and $\boldsymbol{\zeta}^{\mathrm{U}}$ are the sets of constrains and multipliers, respectively.

The solute energy $E^{\mathrm{U}}(\mathbf{C})$ depends on the electronic structure method used, which will be discussed later. The form of the excess chemical potential $\Delta\mu$ depends on the closure employed. Several closures have been proposed and used, and each has its own advantages. Here, we use hypernetted chain (HNC) closures and its nth order partial series expansion. Then, the excess chemical potential is rewritten in Equations (2) and (3), as follows:

$$\begin{aligned}\Delta\mu(\mathbf{C},c,h) &= \sum_{\alpha s}\left(\Delta\mu_{\alpha s}^{\mathrm{HNC}}-\beta^{-1}n_s\int d\mathbf{r}\Theta(h_{\alpha s}(r))\frac{(t_{\alpha s}(r)-\beta u_{\alpha s}(C,\zeta,r))^{n+1}}{(n+1)!}\right)\\ &=\beta^{-1}\sum_{\alpha s}n_s\int d\mathbf{r}\left[(1-\Theta(t_{\alpha s}(r)-\beta u_{\alpha s}(r)))(\exp(t_{\alpha s}(r)-\beta u_{\alpha s}(r)))+\Theta(t_{\alpha s}(r,\lambda)-\beta\lambda u_{\alpha s}(r))\left(\sum_{i=0}^{n}\frac{1}{i!}(t_{\alpha s}(r)-\beta u_{\alpha s}(r))^i\right)-t_{\alpha s}(r)-h_{\alpha s}(r)t_{\alpha s}(r)+\frac{1}{2}h_{\alpha s}^2(r)\right]\\ &-\frac{\beta^{-1}}{(2\pi)^3}\int d\mathbf{k}\left[\frac{1}{2}\sum_{\alpha,s,\gamma,t}\hat{c}_{\alpha s}(k)\hat{c}_{\gamma t}(k)\hat{\omega}_{\alpha\gamma}(k)\hat{X}_{st}(k)-\sum_{\alpha,s}\hat{c}_{\alpha s}(k)\rho_s\hat{h}_{\alpha s}(k)\right],\end{aligned} \tag{2}$$

$$\Delta\mu_{\alpha s}^{\mathrm{HNC}}=\beta^{-1}n_s\int d\mathbf{r}\left(\frac{1}{2}h_{\alpha s}^2(r)-c_{\alpha s}(r)-\frac{1}{2}h_{\alpha s}(r)c_{\alpha s}(r)\right), \tag{3}$$

where Θ is the Heaviside function, β is the inverse temperature, n_s is the number density of site s, and $\Delta\mu_{\alpha s}^{\mathrm{HNC}}$ is the excess chemical potential using the HNC closure. When n is set to 1 in Equation (2), $\Delta\mu$ corresponds to the Kovalenko–Hirata (KH) closure. $\hat{c}$, $\hat{h}$, $\hat{\omega}$, and $\hat{\mathrm{X}}$ denote

1096987x, 2023, 1, Downloaded from https://onlinelibrary.wiley.com/doi/10.1002/jcc.27009 by Kyushu University, Wiley Online Library on [21/11/2022]. See the Terms and Conditions (https://onlinelibrary.wiley.com/terms-and-conditions) on Wiley Online Library for rules of use; OA articles are governed by the applicable Creative Commons License

the direct, total, intramolecular correlation functions and solvent susceptibility in Fourier space. $u_{\alpha s}$ is an interaction potential between solute site α and solvent site s given as

$$u_{\alpha s}(r) = 4\varepsilon_{\alpha s}\left[\left(\frac{\sigma_{\alpha s}}{r}\right)^{12} - \left(\frac{\sigma_{\alpha s}}{r}\right)^{6}\right] + \frac{q_\alpha q_s}{r}, \tag{4}$$

where ε and σ are the Lennard-Jones potential parameters with conventional meanings and q_α and q_s are the effective point charge on solute site α and solvent site s, respectively.

Let us assume the HF method as the electronic structure method used in the RISM-SCF. In the HF method, the molecular orbital (MO) coefficients are the variational parameters, and the orthonormality of MOs is imposed as a constrain. The solute energy E^{U} and the constrains with the multipliers are

$$\begin{aligned} E^{\mathrm{U}} &= \mathrm{tr}\left[(\mathbf{h}^{\mathrm{core}} + \mathbf{F})\mathbf{C}\mathbf{C}^{\dagger}\right] \\ &= \mathrm{tr}\left[(\mathbf{h}^{\mathrm{core}} + \mathbf{F})\mathbf{D}\right], \end{aligned} \tag{5}$$

$$\boldsymbol{\zeta}^{\mathrm{U}} \times \boldsymbol{e}^{\mathrm{U}} = \sum_{pq} \epsilon_{pq}\left(C^{\dagger}SC - I\right)_{pq}, \tag{6}$$

which are common regardless of the relativistic and nonrelativistic cases. Here, matrix $\mathbf{C}$ stores the occupied MO coefficients, $\mathbf{D}$ is the density matrix, and $\mathbf{h}^{\mathrm{core}}$ and $\mathbf{F}$ are the core Hamiltonian and Fock matrices, respectively. Thus, the total Lagrangian of DHF/RISM-SCF can be rewritten as the sum of these terms, as follows.

$$\begin{aligned} L(\mathbf{C}, \boldsymbol{\zeta}_{\mathrm{U}}, c, h, t) \;=\; & \mathrm{tr}\left[(\mathbf{h}^{\mathrm{core}} + \mathbf{F})\mathbf{D}\right] - \sum_{pq} \epsilon_{pq}\left(C^{\dagger}SC - I\right)_{pq} \\ & + \beta^{-1}\sum_{\alpha s} n_s \int \mathrm{d}\mathbf{r}\left[\left(1 - \Theta(t_{\alpha s}(r) - \beta u_{\alpha s}(r))\right)\left(\exp\left(t_{\alpha s}(r) - \beta u_{\alpha s}(r)\right)\right) + \Theta(t_{\alpha s}(r,\lambda) - \beta\lambda u_{\alpha s}(r))\left(\sum_{i=0}^{n} \frac{1}{i!}\left(t_{\alpha s}(r) - \beta u_{\alpha s}(r)\right)^{i}\right) - t_{\alpha s}(r) - h_{\alpha s}(r)t_{\alpha s}(r) + \frac{1}{2}h_{\alpha s}^{2}(r)\right] \\ & - \frac{\beta^{-1}}{(2\pi)^3}\int \mathrm{d}\mathbf{k}\left[\frac{1}{2}\sum_{\alpha,s,\gamma,t} \widehat{c}_{\alpha s}(k)\widehat{c}_{\gamma t}(k)\widehat{\omega}_{\alpha\gamma}(k)\widehat{\mathrm{X}}_{st}(k) - \sum_{\alpha,s} \widehat{c}_{\alpha s}(k)\rho_s \widehat{h}_{\alpha s}(k)\right]. \end{aligned} \tag{7}$$

Taking variations of the Lagrangian with respect to the correlation functions $c_{\alpha s}$, $h_{\alpha s}$, and $t_{\alpha s}$ and MO coefficients $\mathbf{C}$, the stationary conditions for RISM-SCF can be obtained. The resulting equations obtained from the variations with respect to $c_{\alpha s}$, $h_{\alpha s}$, and $t_{\alpha s}$ are the RISM equations: the relational equation between the total, direct, and indirect correlation functions, and the closure equation. The equation obtained from the variation with respect to $\mathbf{C}$ is the RISM-SCF equation describing the electronic structure of the solute molecule surrounded by solvent:

$$\frac{\partial L}{\partial \mathbf{C}^{\dagger}} = \left(\frac{\delta E^{\mathrm{U}}}{\delta \mathbf{D}} + \frac{\delta \Delta\mu}{\delta \mathbf{D}}\right)\frac{\delta \mathbf{D}}{\delta \mathbf{C}^{\dagger}} - \mathbf{S}\mathbf{C}\epsilon = \left(\frac{\delta E^{\mathrm{U}}}{\delta \mathbf{D}} + \frac{\delta \Delta\mu}{\delta \mathbf{D}}\right)\mathbf{C} - \mathbf{S}\mathbf{C}\epsilon = \mathbf{0}, \tag{8}$$

where, for later convenience, the variation is taken with respect to $\mathbf{C}^{\dagger}$ instead of $\mathbf{C}$. The variation of E^{U} with respect to the density matrix gives the Fock matrix in gas phase:

$$\frac{\delta E^{\mathrm{U}}}{\delta \mathbf{D}} = \mathbf{F}^{\mathrm{gas}} = \mathbf{h}^{\mathrm{core}} + \mathbf{J} - \mathbf{K}, \tag{9}$$

$$J_{\mu\nu} = \sum\nolimits_{lk} D_{\sigma\lambda}(\mu\nu|\lambda\sigma), \tag{10}$$

$$K_{\mu\nu} = \sum\nolimits_{\sigma\lambda} D_{\sigma\lambda}(\mu\sigma|\lambda\nu), \tag{11}$$

where $\mathbf{J}$ and $\mathbf{K}$ are the Coulomb and exchange integral matrices, respectively. The variation of $\Delta\mu$ with respect to the density matrix $\mathbf{D}$ can be rewritten via the potential $u_{\alpha s}$ and the charges on the solute site, α, q_α:

$$\begin{aligned} \frac{\delta \Delta\mu}{\delta \mathbf{C}^{\dagger}} &= \sum\nolimits_{\alpha s} \frac{\delta \Delta\mu}{\delta u_{\alpha s}} \frac{\partial u_{\alpha s}}{\partial q_\alpha} \frac{\delta q_\alpha}{\delta \mathbf{D}} \frac{\partial \mathbf{D}}{\partial \mathbf{C}^{\dagger}} = \sum\nolimits_{\mu\alpha s} q_s \int \mathrm{d}\mathbf{r} \frac{h_{\alpha s}(r) + 1}{r} b_{\nu\mu,\alpha} C_{\mu i} \\ &= \sum\nolimits_{\alpha\mu} V_\alpha b_{\nu\mu,\alpha} C_{\mu i}, \end{aligned} \tag{12}$$

$$V_\alpha = \sum\nolimits_s \frac{\delta \Delta\mu}{\delta u_{\alpha s}} \frac{\partial u_{\alpha s}}{\partial q_\alpha} = \sum\nolimits_s q_s \int \mathrm{d}\mathbf{r} \frac{h_{\alpha s}(r) + 1}{r}, \tag{13}$$

where $b_{\mu\nu,\alpha}$ is the matrix representation of the population operator for the solute site α.

In the following, we use the relativistic four-component function as the HF wave function and derive the specific RISM-SCF equation.

In the four-component method, MOs are expressed by large and small component spinors:

$$\phi_i = \begin{pmatrix} \phi_i^{\mathrm{L}} \\ \phi_i^{\mathrm{S}} \end{pmatrix}, \tag{14}$$

where each component is expanded by the χ basis spinors for each component:

$$\phi^{\mathrm{L}} = \sum\nolimits_\mu c_{\mu i}^{\mathrm{L}} \chi_\mu^{\mathrm{L}}, \phi^{\mathrm{S}} = \sum_\mu c_{\mu i}^{\mathrm{S}} \chi_\mu^{\mathrm{S}}. \tag{15}$$

The four-component matrices can be expressed as

1096987x, 2023, 1, Downloaded from https://onlinelibrary.wiley.com/doi/10.1002/jcc.27009 by Kyushu University, Wiley Online Library on [21/11/2022]. See the Terms and Conditions (https://onlinelibrary.wiley.com/terms-and-conditions) on Wiley Online Library for rules of use; OA articles are governed by the applicable Creative Commons License

$$\mathbf{D}=\begin{bmatrix}\mathbf{D}^{\mathrm{LL}} & \mathbf{D}^{\mathrm{LS}}\\ \mathbf{D}^{\mathrm{SL}} & \mathbf{D}^{\mathrm{SS}}\end{bmatrix}, \tag{16}$$

$$D_{\mu\nu}^{\mathrm{XY}}=\sum\nolimits_i C_{\mu i}^{\mathrm{X}}\left(C_{\nu i}^{\mathrm{Y}}\right)^{*}, \tag{17}$$

$$\mathbf{h}^{\mathrm{core}}=\begin{bmatrix}\mathbf{V}^{\mathrm{LL}} & \boldsymbol{\Pi}^{\mathrm{LS}}\\ \boldsymbol{\Pi}^{\mathrm{SL}} & \mathbf{V}^{\mathrm{SS}}-2c^2\mathbf{S}^{\mathrm{SS}}\end{bmatrix}, \tag{18}$$

$$V_{\mu\nu}^{\mathrm{XX}}=\langle\chi_\mu^{\mathrm{X}}|V|\chi_\nu^{\mathrm{X}}\rangle, \tag{19}$$

$$\Pi_{\mu\nu}^{\mathrm{XY}}=\langle\chi_\mu^{\mathrm{X}}|c\boldsymbol{\sigma}\cdot\mathbf{p}|\chi_\nu^{\mathrm{Y}}\rangle, \tag{20}$$

$$S_{\mu\nu}^{\mathrm{XX}}=\langle\chi_\mu^{\mathrm{X}}|\chi_\nu^{\mathrm{X}}\rangle, \tag{21}$$

$$\mathbf{J}=\begin{bmatrix}\mathbf{J}^{\mathrm{LL}} & 0\\ 0 & \mathbf{J}^{\mathrm{SS}}\end{bmatrix}, \tag{22}$$

$$J_{\mu\nu}^{\mathrm{XX}}=\sum\nolimits_{\sigma\lambda}D_{\sigma\lambda}^{\mathrm{LL}}\left(\chi_\mu^{\mathrm{X}}\chi_\nu^{\mathrm{X}}|\chi_\lambda^{\mathrm{L}}\chi_\sigma^{\mathrm{L}}\right)+D_{\sigma\lambda}^{\mathrm{SS}}\left(\chi_\mu^{\mathrm{X}}\chi_\nu^{\mathrm{X}}|\chi_\lambda^{\mathrm{S}}\chi_\sigma^{\mathrm{S}}\right), \tag{23}$$

$$\mathbf{K}=\begin{bmatrix}\mathbf{K}^{\mathrm{LL}} & \mathbf{K}^{\mathrm{LS}}\\ \mathbf{K}^{\mathrm{SL}} & \mathbf{K}^{\mathrm{SS}}\end{bmatrix}, \tag{24}$$

$$K_{\mu\nu}^{\mathrm{XY}}=\sum\nolimits_{\sigma\lambda}D_{\sigma\lambda}^{\mathrm{XY}}\left(\chi_\mu^{\mathrm{X}}\chi_\sigma^{\mathrm{X}}|\chi_\lambda^{\mathrm{Y}}\chi_\nu^{\mathrm{Y}}\right). \tag{25}$$

The charge q_α on solute site α in Equation (12) is determined by the electrostatic potential (ESP) method,[33,34] so as to reproduce the electrostatic potential due to the solute electron and nuclei.

The vector $\mathbf{q}$ storing the point charges q_α as elements is then given by

$$\begin{aligned}\mathbf{q}=&\mathrm{Tr}\left[\mathbf{D}^{\mathrm{LL}}\left(\mathbf{a}^{-1}\mathbf{B}^{\mathrm{LL}}-\frac{\left(\mathbf{1}^{\mathrm{t}}\mathbf{a}^{-1}\mathbf{B}^{\mathrm{LL}}-\mathbf{S}^{\mathrm{LL}}\right)}{\mathbf{1}^{\mathrm{t}}\mathbf{a}^{-1}\mathbf{1}}\mathbf{a}^{-1}\mathbf{1}\right)\right]\\&+\mathrm{Tr}\left[\mathbf{D}^{\mathrm{SS}}\left(\mathbf{a}^{-1}\mathbf{B}^{\mathrm{SS}}-\frac{\left(\mathbf{1}^{\mathrm{t}}\mathbf{a}^{-1}\mathbf{B}^{\mathrm{SS}}-\mathbf{S}^{\mathrm{SS}}\right)}{\mathbf{1}^{\mathrm{t}}\mathbf{a}^{-1}\mathbf{1}}\mathbf{a}^{-1}\mathbf{1}\right)\right].\end{aligned} \tag{26}$$

$$a_{\alpha\beta}=\int\mathrm{d}\mathbf{r}\frac{1}{|\mathbf{r}-\mathbf{R}_\alpha||\mathbf{r}-\mathbf{R}_\beta|}, \tag{27}$$

$$B_{\mu\nu}^{\mathrm{XX}}=\int\mathrm{d}\mathbf{r}\frac{1}{|\mathbf{r}-\mathbf{R}_\alpha|}\int\mathrm{d}\mathbf{r}'\chi_\mu^{\mathrm{X}*}(\mathbf{r}')\frac{1}{|\mathbf{r}-\mathbf{r}'|}\chi_\nu^{\mathrm{X}}(\mathbf{r}'). \tag{28}$$

The variation of the site charge, Equation (26), with respect to the density matrix gives the solvation potential matrix for solute site α:

$$\frac{\delta q_\alpha}{\delta\mathbf{D}}=\begin{bmatrix}\mathbf{b}_\alpha^{\mathrm{LL}} & \mathbf{0}\\ \mathbf{0} & \mathbf{b}_\alpha^{\mathrm{SS}}\end{bmatrix}, \tag{29}$$

where

$$\mathbf{b}^{\mathrm{XX}}=\mathbf{a}^{-1}\mathbf{B}^{\mathrm{XX}}-\frac{\left(\mathbf{1}^{\mathrm{t}}\mathbf{a}^{-1}\mathbf{B}^{\mathrm{XX}}-\mathbf{S}^{\mathrm{XX}}\right)}{\mathbf{1}^{\mathrm{t}}\mathbf{a}^{-1}\mathbf{1}}\mathbf{a}^{-1}\mathbf{1}. \tag{30}$$

The solvation Fock matrix is defined as the sum of the gas-phase Fock matrix and solvation potential matrix:

$$\mathbf{F}^{\mathrm{solv}}=\begin{bmatrix}\mathbf{F}^{\mathrm{LL,gas}}+\mathbf{V}^{\mathrm{LL,solv}} & \mathbf{F}^{\mathrm{LS,gas}}\\ \mathbf{F}^{\mathrm{SL,gas}} & \mathbf{F}^{\mathrm{SS,gas}}+\mathbf{V}^{\mathrm{SS,solv}}\end{bmatrix}, \tag{31}$$

where

$$\mathbf{V}^{\mathrm{XX,solv}}=\sum\nolimits_\alpha V_\alpha\mathbf{b}_\alpha^{\mathrm{XX}}. \tag{32}$$

Thus, we finally obtain the DHF/RISM-SCF equation as an eigenvalue problem:

$$\mathbf{F}^{\mathrm{solv}}\mathbf{C}=\mathbf{S}\mathbf{C}\boldsymbol{\epsilon}. \tag{33}$$

Due to the variational formalism, energy derivatives, in particular first-order derivatives, can be concise, as shown by Sato et al.[31] The first-order derivative of the Helmholtz energy with respect to the solute molecular coordinates $\mathbf{R}_a$ is expressed simply as

$$\begin{aligned}\frac{\partial A}{\partial\mathbf{R}_a}=&\frac{\partial E^{\mathrm{U}}}{\partial\mathbf{R}_a}+\frac{1}{2\beta(2\pi)^3}\sum_{\alpha\gamma st}\int d\mathbf{k}\hat{c}_{\alpha s}(k)\hat{c}_{\gamma t}(k)\frac{\partial\hat{\omega}_{\alpha\gamma}(k)}{\partial\mathbf{R}_A}\hat{\mathrm{X}}_{st}(k)\\&+\sum\nolimits_\alpha V_\alpha\mathrm{tr}\left(\mathbf{D}\frac{\partial\mathbf{b}_\alpha}{\partial\mathbf{R}_A}\right).\end{aligned} \tag{34}$$

TABLE 1 LJ parameters of solute and solvent sites used in the reference interaction-site model self-consistent field (RISM-SCF) calculations

	σ (Å)	ε (kcal/mol)	q (e)[a]
I^- and CH_3I			
C	3.3997	0.1094	–
H	2.4714	0.0157	–
I	3.8309	0.5	–
H_2X (X = O–Po)			
H (expect for H_2Po)	1.0000	0.056	–
H (for H_2Po)	2.886	0.325	–
O	3.166	0.1554	–
S	4.035	0.274	–
Se	4.205	0.291	–
Te	4.009	0.339	–
Po	4.709	0.325	–
Solvent water			
O	3.166	0.1554	−0.8476
H	1.0000	0.056	0.4238

[a]The partial charges on solute sites are determined as a result of the RISM-SCF calculation.

1096987x, 2023, 1, Downloaded from https://onlinelibrary.wiley.com/doi/10.1002/jcc.27009 by Kyushu University, Wiley Online Library on [21/11/2022]. See the Terms and Conditions (https://onlinelibrary.wiley.com/terms-and-conditions) on Wiley Online Library for rules of use; OA articles are governed by the applicable Creative Commons License

The first term of the right-hand side of Equation (34) corresponds to the change in the solute electronic energy; the second term corresponds to the change in the solute–solvent distribution function due to the modification of the intramolecular correlation; and the last term corresponds to the change in partial charge on solute sites. The analytical energy gradients for the four-component relativistic DHF/RISM-SCF are obtained by replacing the nonrelativistic molecular integral with four-component ones.

It should be noted that, although not treated in the present paper, it is straightforward to extend the method to the four-component Dirac–Kohn–Sham (DKS) density functional method. The four-component DKS/RISM-SCF equation can be obtained by replacing the solute DHF energy expression with the DKS energy expression:

$$E^{U} = E^{DKS} = \mathrm{tr}[\mathbf{D}(\mathbf{h}^{core} + \mathbf{J} - \gamma\mathbf{K})] + e^{XC}(\rho), \quad (35)$$

where γ is the parameter defining the weight of the Hartree–Fock exchange, and e^{XC} is an exchange-correlation functional. Thus, the solvation Fock corresponding to the DKS/RISM-SCF is the sum of the four-component Kohn–Sham matrix and the solvation potential matrix multiplied by V_α.

3 | COMPUTATIONAL DETAILS

To demonstrate the present method, we applied it to the ground states of the I^- ion, to methyl iodide CH_3I, and to hydrogen chalcogenides H_2X (X = O, S, Se, Te, and Po) in aqueous solution. The basis sets used in the DHF calculations were the uncontracted correlation-consistent valence triple zeta (cc-pVTZ) basis set for C, H, O, and S,[35,36] and the uncontracted Dyall's triple zeta plus polarization (TZP) basis set for Se, Te, I, and Po.[37] The geometries of CH_3I and H_2X in the solution were optimized at the DHF/RISM-SCF level.

The parameters used in the RISM-SCF method were as follows: The temperature and density of solvent water were 298 K and 0.03334 molecules/Å^3, respectively. The LJ parameters σ and ε for the solute and solvent sites are listed in Table 1.[38] For H_2Po, the LJ parameters for the H of silane (H_4Si) were used[39] to ensure proper charge polarization between H and Po. The transferable intermolecular potential with three points (TIP3P) parameter set[40] for the geometrical and potential parameters for solvent water was used with modified H parameters. There were 2048 grid points with a spacing of 0.05 Å for pair correlation functions in the RISM calculations. PCM-SCF calculations were performed by DIRAC19.[41,42]

4 | APPLICATIONS

4.1 | The iodine ion (I^-) and methyl iodide (CH_3I)

The electronic structure and solvation structure of the iodine ion (I^-) and methyl iodide (CH_3I) were evaluated by the relativistic and

TABLE 3 Optimized geometrical parameters, *z* component of electric dipole moment, and ESP charge for CH_3I

	Relativistic		Nonrelativistic	
	GAS	RISM	GAS	RISM
r(C–I) (Å)	2.143	2.155	2.144	2.157
r(C–H) (Å)	1.075	1.073	1.075	1.073
∠ICH (°)	107.5	106.6	107.7	106.7
DM(*z*) (a.u.)	−0.763	−1.080	−0.821	−1.155
q_I (*e*)	−0.128	−0.185	−0.146	−0.210
q_C (*e*)	−0.402	−0.495	−0.344	−0.378
q_H (*e*)	0.177	0.226	0.164	0.196

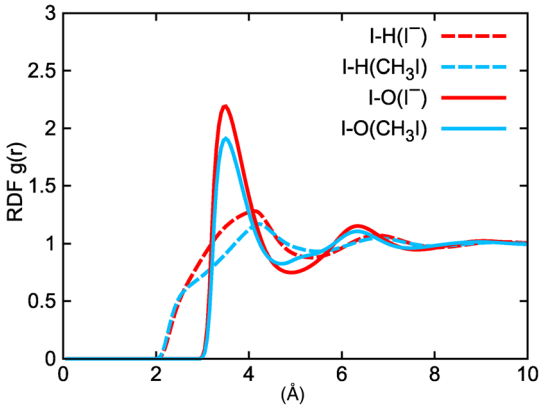

FIGURE 1 Radial distribution functions between the I atom and solvent water

TABLE 2 Helmholtz energy and solvation free energy for I^- and CH_3I, and their component decomposition

	I^-		CH_3I	
	Relativistic	Nonrelativistic	Relativistic	Nonrelativistic
A (Hartree)	−7116.25060	−6918.21333	−7155.65459	−6957.60014
E^U	−7116.11102	−6918.07374	−7155.67243	−6957.61794
$\Delta\mu$	−0.13959	−0.13959	0.01784	0.01780
A^{slv} (kcal/mol)	−87.59	−87.59	11.96	12.00
$\Delta\mu^{NES}$	7.30	7.30	14.40	14.41
$\Delta\mu^{ES}$	−94.89	−94.89	−3.21	−3.24
E^{reorg}	$<10^{-3}$	$<10^{-3}$	0.76	0.83

1096987x, 2023, 1, Downloaded from https://onlinelibrary.wiley.com/doi/10.1002/jcc.27009 by Kyushu University, Wiley Online Library on [21/11/2022]. See the Terms and Conditions (https://onlinelibrary.wiley.com/terms-and-conditions) on Wiley Online Library for rules of use; OA articles are governed by the applicable Creative Commons License

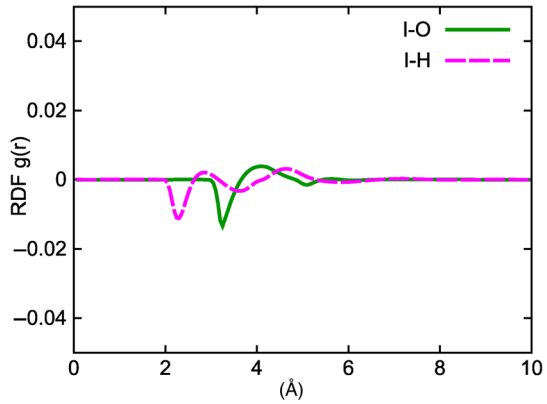

FIGURE 2 Difference between the relativistic and nonrelativistic radial distribution functions for CH_3I

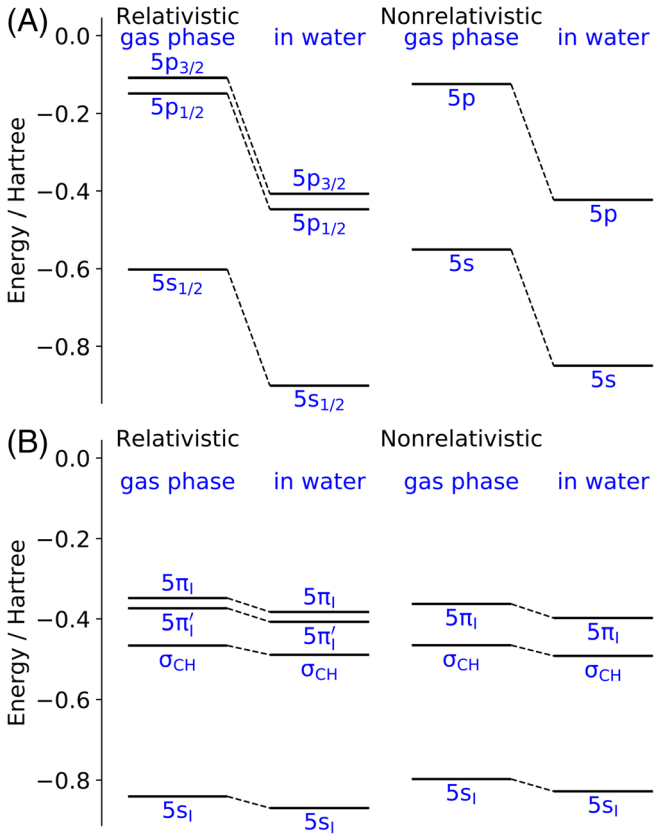

FIGURE 3 Energy levels of (A) 5p orbitals of I^- and (B) 5p orbitals of I in CH_3I

nonrelativistic HF/RISM-SCF methods. In Table 2, the Helmholtz energy and its components obtained by relativistic and nonrelativistic method for I^- and CH_3I are compared.

The solvation free energy (SFE) A^{slv} in the RISM-SCF method is defined as the difference between the Helmholtz energy in solution phase A and the energy in gas phase E^{gas}:

$$A^{slv} = A - E^{gas} = E^{U} - E^{gas} + \Delta\mu. \tag{36}$$

TABLE 4 Optimized geometrical parameters for H_2X (X = O–Po)

	GAS		RISM		PCM	
X	r (Å)	θ (°)	r (Å)	θ (°)	r (Å)	θ (°)
O	0.940	105.9	0.945	105.6	0.944	104.9
S	1.329	94.1	1.330	96.1	1.331	94.9
Se	1.451	92.9	1.449	95.2	1.452	93.7
Te	1.649	92.1	1.645	93.9	1.649	92.6
Po	1.742	90.7	1.742	90.3	1.746	90.0

The energy difference, $E^{U} - E^{gas}$, in the right-hand side can be regarded as the electronic reorganization energy E^{reorg} due to the solvation, and the excess chemical potential $\Delta\mu$ can be divided into the electrostatic $\Delta\mu^{ES}$ and the nonelectrostatic $\Delta\mu^{NES}$ components; hence, A^{slv} is further rewritten as

$$A^{slv} = E^{reorg} + \Delta\mu^{ES} + \Delta\mu^{NES}. \tag{37}$$

As shown in Table 2, I^- is strongly stabilized due to the solvation because of its ionic nature. The major contribution to this stabilization is the electrostatic interaction with the solvent water. Since I^- consists of only one site, all the electron charges are assigned to the single site. As a result, the solute–solvent interaction potential for the RISM calculation is the same in both relativistic and nonrelativistic calculations. Therefore, the SFE values are identical in both cases. By contrast, the SFE of CH_3I, a polyatomic molecule, is affected by the relativistic effects. In the DHF/RISM-SCF framework, the relativistic effects on electronic states of the solute molecule influence the solute–solvent interactions through effective charges on solute atoms. Moreover, the solvation structure changed by relativistic effects also affects the electron reorganization energy of the solute molecule. In the present calculation, the relativistic effects seem to suppress the electrostatic interaction between solute and solvent molecules and therefore the magnitude of all the SFE components becomes smaller than those of nonrelativistic results. Consequently, the total SFE of the relativistic calculation, 11.96 kcal/mol, was slightly lower than the nonrelativistic one, 12.00 kcal/mol. The optimized molecular structure and electrical properties of solute CH_3I are summarized in Table 3. As can be seen in the table, the C–I distance and the dipole moment of the solute CH_3I become smaller due to the relativistic effects. Such structural and electrostatic character weakens the solute–solvent interactions.

The radial distribution functions (RDFs)[27] between the I ion/atom of the solute and the O and H atoms of the solvent by DHF/RISM-SCF are shown in Figure 1. For I^-, the RDF for I–O has a sharp high peak at $r = 3.4$ Å and the RDF for I–H has a sharp high peak at $r = 2.15$ Å and a relatively low peak at $r = 4.15$ Å. In CH_3I, the RDF for I–O has a high peak at $r = 3.50$ Å, and the RDF for I–H has a shoulder around $r = 2.70$ Å and a peak at $r = 4.20$ Å. These peaks and the shoulder correspond to water molecules in the first solvation shell.

1096987x, 2023, 1, Downloaded from https://onlinelibrary.wiley.com/doi/10.1002/jcc.27009 by Kyushu University, Wiley Online Library on [21/11/2022]. See the Terms and Conditions (https://onlinelibrary.wiley.com/terms-and-conditions) on Wiley Online Library for rules of use; OA articles are governed by the applicable Creative Commons License

TABLE 5 Helmholtz energy and solvation free energy for H_2X (X = O–Po), and their component decomposition

	H_2O		H_2S		H_2Se		H_2Te		H_2Po	
	RISM	PCM	RISM	PCM	RISM	PCM	RISM	PCM	RISM	PCM
A (Hartree)	−76.1209	−76.1218	−399.8201	−399.8352	−2429.7964	−2429.8143	−6795.0666	−6795.0840	−22238.6862	−22238.7121
E^U	−76.1041	−76.1118	−399.8269	−399.8306	−2429.8077	−2429.8106	−6795.0794	−6795.0813	−22238.7099	−22238.7093
$\Delta\mu$	−0.0167	−0.0100	0.0068	−0.0046	0.0113	−0.0037	0.0127	−0.0027	0.0237	−0.0028
A^{slv} (kcal/mol)	−5.31	−5.61	6.95	−2.53	9.13	−2.06	8.78	−1.59	14.94	−1.61
$\Delta\mu^{NES}$	6.82	-	10.48	-	11.27	-	9.46	-	15.07	-
$\Delta\mu^{ES}$	−18.17	−6.28	−6.36	−2.90	−4.38	−2.32	−1.67	−1.72	−0.22	−1.75
E^{reorg}	6.04	0.67	2.83	0.37	2.24	0.25	0.99	0.13	0.09	0.14

The peaks of CH_3I are featured to be lower and broader than those of I^-. These results indicate tight hydration around the charged I^- ion and loose hydration around I of the neutral molecule CH_3I.

The difference between the RDFs of CH_3I by the relativistic and nonrelativistic RISM-SCF is shown in Figure 2. The RDFs of I^- are not shown because they are identical for relativistic and nonrelativistic, as discussed above. From the figure, the first peak height of the RDF in the relativistic case is slightly lower than in the nonrelativistic case. This feature corresponds to the SFE behavior discussed above; that is, the introduction of the relativistic effects weakens the solute–solvent interaction.

In contrast to the solvation structures, which differ little between the relativistic and nonrelativistic cases, the electronic structures of I^- and CH_3I are naturally different due to the relatively large spin–orbit interaction. Figure 3A,B presents the energy levels of the four highest energy orbitals (including degeneracy) of I^- and CH_3I, respectively. In the charged system I^-, the $5p_{3/2}$, $5p_{1/2}$ and 5s orbitals are significantly stabilized by −0.2989 a.u. The MOs of CH_3I corresponding to these orbitals of I^- are the highest occupied MO (HOMO) (9e; characterized as $5\pi_I$), HOMO−1 ($9e'; 5\pi_I'$), HOMO−2 ($13a_1$; σ_{CH}), and HOMO−5 ($12a_1$; $5s_I$). The stabilizations of these energy levels are relatively small, namely: −0.0346, −0.0338, −0.0230, and −0.0290 a.u., respectively, as expected for a neutral molecule.

4.2 | Hydrogen chalcogenide H_2X (X = O, S, Se, Te, and Po)

Another example is the series of hydrogen chalcogenides. The molecular structures of the H_2X molecules in gas phase and in water, which were optimized using the DHF/RISM-SCF and DHF/PCM-SCF methods, are shown in Table 4. These molecules have also been examined in the relativistic PCM-SCF paper.[23] This paper reported that bond lengths increase monotonically with increasing chalcogen atomic number in correlation with the size of the central atom, and that there is no deviation from this trend even when relativity is included and the solvent effect is considered. The DHF/RISM-SCF method provides similar results. The structures by DHF/RISM-SCF and DHF/PCM-SCF methods in the table are quite close, with a maximum difference of 0.04 Å in bond distance and 2.5° in bond angle. For the bond distance, the DHF/RISM-SCF method tends to have a slightly larger distance, and for the bond angle, the DHF/RISM-SCF method tends to have a slightly smaller angle. The solvent effect on the solute structure was smaller with the DHF/RISM-SCF method than with DHF/PCM-SCF. In fact, even for H_2O, where the change in electric dipole moment due to solvation, as will be shown later, is large: the changes are +0.005 Å for bond distance and −0.3° for bond angle. This is much the same for the DHF/PCM-SCF method.

The Helmholtz energies, as well as the SFEs and their components, for H_2X (X = O, S, Se, Te, and Po) are shown in Table 5. The Helmholtz energies and SFEs by the DHF/PCM-SCF method are also listed. The nonelectrostatic contributions to the SFEs were not included because the nonelectrostatic energy is not handled in the current PCM implementation of the program package (DIRAC). Hence,

1096987x, 2023, 1, Downloaded from https://onlinelibrary.wiley.com/doi/10.1002/jcc.27009 by Kyushu University, Wiley Online Library on [21/11/2022]. See the Terms and Conditions (https://onlinelibrary.wiley.com/terms-and-conditions) on Wiley Online Library for rules of use; OA articles are governed by the applicable Creative Commons License

the SFEs by the DHF/PCM-SCF method are the sum of E^{reorg} and $\Delta\mu^{ES}$. For this reason, direct comparison between the total SFEs A^{slv} by the DHF/PCM-SCF and DHF/RISM-SCF methods is not appropriate, and only the electrostatic and electronic reorganization energies are compared below. Table 6 lists the *z* components of the electric dipole moments and the electrostatic potential (ESP) charge on the X atom of the solute molecule. The H_2X molecules have a C_{2v} symmetry, and thus only the *z* component of the dipole moment has a value.

TABLE 6 *Z* component of electric dipole moment and electrostatic potential charge on X for H_2X (X = O–Po)

	H_2O	H_2S	H_2Se	H_2Te	H_2Po
GAS					
DM(z) (a.u.)	0.781	0.449	0.307	0.115	−0.229
q (*e*)	−0.741	−0.319	−0.226	−0.116	0.033
RISM					
DM(z) (a.u.)	1.137	0.861	0.732	0.464	−0.342
q (*e*)	−1.056	−0.553	−0.446	−0.268	0.080
PCM[a]					
DM(z) (a.u.)	0.903	0.584	0.426	0.191	−0.327

[a]Reference 23.

The SFE by the DHF/RISM-SCF method is negative (−5.31 kcal/mol) for H_2O and positive (6.95–14.94 kcal/mol) for the other molecules, increasing with the atomic number of chalcogen. The electrostatic and nonelectrostatic components of the SFE increase from H_2O to H_2Po: the electrostatic component increases from −18.17 kcal/mol for H_2O to −0.22 for H_2Po, and the nonelectrostatic component increases from 6.82 kcal/mol for H_2O to 15.07 for H_2Po. By contrast, the reorganization energy is smaller than these two energies, decreasing from 6.04 to 0.99 kcal/mol. According to Table 6, the magnitude of the electric dipole moment and ESP charge decrease with increasing chalcogen atomic number, indicating that the polarity of the molecules reduces with increasing chalcogen atomic number. The SFE results correspond to the magnitude of the molecular polarity. That is, the larger the polarity of the molecule, the larger the magnitude of the electrostatic component and the reorganization energy, and the smaller the magnitude of the nonelectrostatic component. For H_2O, the most polar molecule, the electrostatic component of −18.17 kcal/mol is dominant, and the nonelectrostatic component and reorganization energy are of similar magnitude, 6.82 and 6.04 kcal/mol, respectively. By contrast, for H_2Po, the least polar molecule, the nonelectrostatic

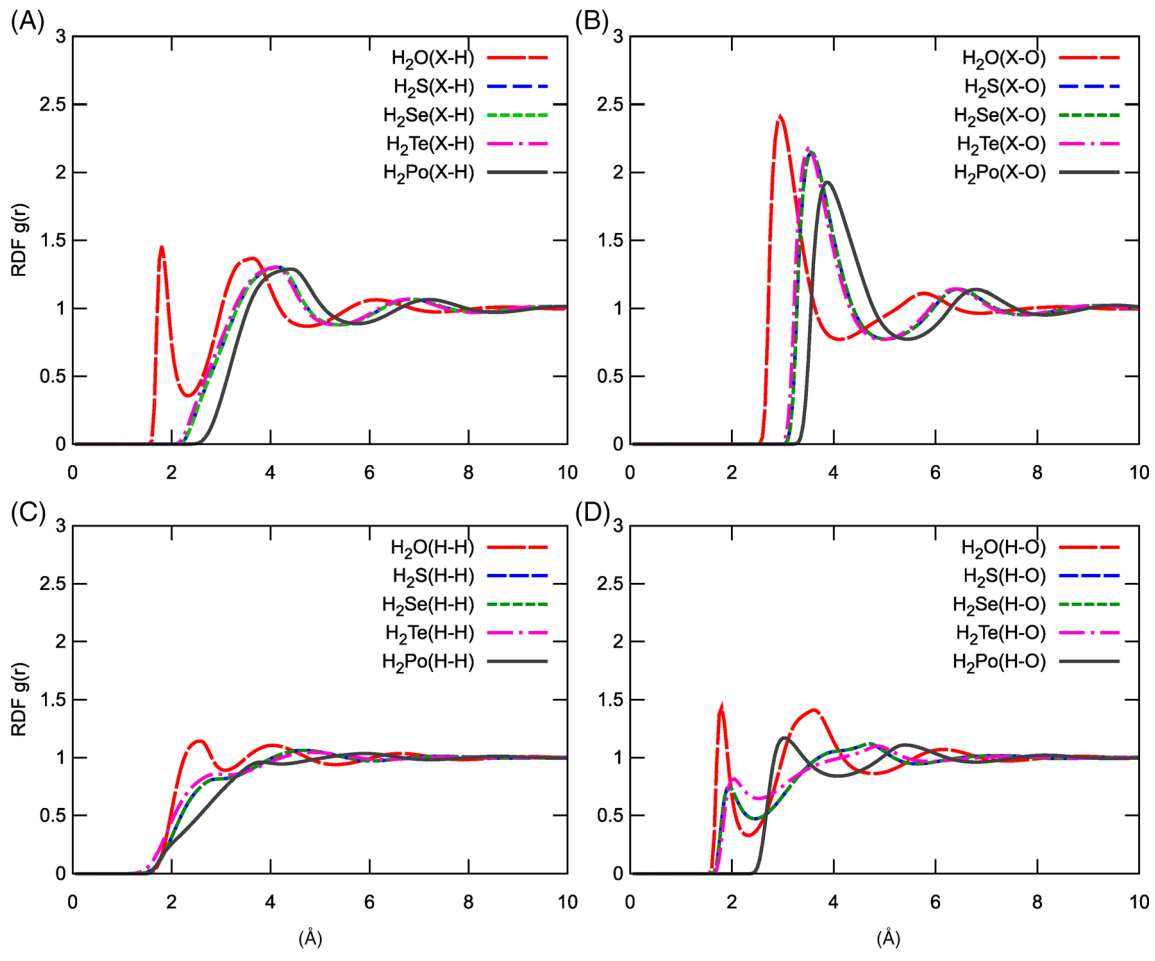

FIGURE 4 Radial distribution functions between H_2X and solvent water

1096987x, 2023, 1, Downloaded from https://onlinelibrary.wiley.com/doi/10.1002/jcc.27009 by Kyushu University, Wiley Online Library on [21/11/2022]. See the Terms and Conditions (https://onlinelibrary.wiley.com/terms-and-conditions) on Wiley Online Library for rules of use; OA articles are governed by the applicable Creative Commons License

energy of 15.07 kcal/mol is dominant, and the electrostatic component and reorganization energy are very small, −0.22 and 0.09 kcal/mol, respectively. Both the electrostatic component and reorganization energy are rather smaller by the DHF/PCM-SCF method than by the DHF/RISM-SCF method. Even for H_2O, which has the largest magnitude, the electrostatic component and reorganization energy are −6.28 and 0.67 kcal/mol, respectively. Note that comparing the dipole moments of RISM and PCM in Table 6, the DHF/RISM-SCF values are larger than those of DHF/PCM-SCF. The maximum difference is 0.306 a.u. for H_2Se, while the difference is relatively small for H_2Po with different polarity, 0.015 a.u. The overestimation may be attributed to the fact that the RISM-SCF method overestimates the polarization of solute molecules in polar solvents when using the point-charge representation.[43]

The RDFs by the DHF/RISM-SCF method are shown in Figure 4A–D. The RDFs of H_2S, H_2Se, and H_2Te were similar, indicating that the RDF features can be classified into three groups: H_2O, H_2S–H_2Te, and H_2Po. In all the RDFs, the peak heights decrease with increasing chalcogen atomic number. This reflects the fact that the solute–solvent interaction weakens with increasing chalcogen atomic number, as can be seen from the polarity of the solute molecules in Table 6.

The RDF, g_{X-H}, between X of the solute and H of the solvent (Figure 4A) shows a conspicuous peak at 1.80 Å for H_2O, but there are no corresponding peaks for the other molecules; the second peak for H_2O corresponds to the first peaks of the other molecules. These first peaks are at shorter distances than the first RDF peak between X of the solute and O of the solvent (Figure 4B) in the case of H_2O–H_2Te, and at about the same distance for H_2Po. This indicated that for H_2O, there is distinct hydrogen bond formation between O of the solute and H of the solvent; for H_2Po, the solvent waters take a nearly random orientation with respect to Po; and for H_2S, H_2Se, and H_2Te, the solvent waters are roughly oriented with H toward the X of the solute.

For the four molecules H_2O–H_2Te the RDFs, g_{H-O}, between H of the solutes and O of the solvent in Figure 4D have a peak at about 2 Å, and the RDFs, g_{H-H}, between H of the solute and H of the solvent in Figure 4C have a peak or shoulder at about 2.5 Å. These indicate the hydrogen bond formation between solute H and solvent O for the three molecules. In contrast, there is no peak at a similar position in H_2Po, and g_{H-O} has a small peak around $r = 3.1$ Å, indicating that H of the solute and O of solvent are loosely bound without forming an obvious hydrogen bond.

5 | CONCLUSIONS

We have presented the DHF/RISM-SCF method, which is the initial implementation of a combined method of a four-component relativistic theory and an integral equation theory of molecular liquid to consider both the relativistic and the solvent effects on the electronic structure of solvated molecules. The method was formulated as a variational form of the Helmholtz energy, and the analytic energy gradients were also derived using the variational property.

We have applied the DHF/RISM-SCF method to iodine ion I^-, methyl iodide CH_3I, and hydrogen chalcogenide H_2X (X = O–Po) in aqueous solutions. For I^- and CH_3I, the SFEs and their components, and the RDFs of solvent around the I atoms were shown and discussed. For species with no or small charge bias, the absolute reorganization energy was very small, and the signs of the SFEs were determined by the electrostatic energy in $\Delta\mu$ for I^- and by the nonelectrostatic energy in $\Delta\mu$ for CH_3I. The solvation structures for I^- and CH_3I around the I atom were similar for the peak and shoulder positions, whereas the peak heights were different due to the charge differences. The comparison with the nonrelativistic HF/RISM-SCF results indicated that changes in solvation structure due to relativistic effects were relatively small. In contrast, for the electronic structures of solute, such as the orbital energy levels, the relativistic description using the DHF/RISM-SCF method was essential. For H_2X, the molecular structures, SFE and their components, the electric dipole moment and ESP charges of the solute, and the RDF of solvent around the X and H atoms were computed and discussed focusing mainly on the differences due to the heavy atom X. As shown by the dipole moment results, the polarity of molecule decreased with increasing chalcogen atomic number. Consequently, the SFE increased, and the electrostatic energy decreased in its absolute value. The solvation structures of H_2X were classified into three groups: H_2O, H_2S–H_2Te, and H_2Po. In H_2O, both the O and H atoms formed hydrogen bonds with solvent water. In H_2Po, by contrast, the solvent water took nearly random orientations around the Po atom of the solute. The H atom of the solute and the O atom of the solvent were loosely bound without forming an obvious hydrogen bond. In other molecules, hydrogen bond formation was observed between the H of the solute and the O atom of the solvent, and the solvent waters were roughly oriented with the H atom toward the heavy element of the solute. Overall, it can be said that the DHF/RISM-SCF method appropriately introduces solvent effects to the four-components relativistic electronic structure theory.

The present DHF/RISM-SCF method can be extended in both the four-component relativistic electronic structure theory of solute molecules and the solvent model. Though the electron correlation effect is not so large for the molecular systems treated in the present article, the combination with electron correlation methods is crucial, especially for the precise description of the electronic structure of solute molecules, the quantitative description of chemical reactions, and their application to quasidegenerate systems. For full variational electronic structure methods, such as the four-component KS-DFT and MCSCF methods, the variational approach to the Helmholtz energy is applicable, as described in the Methods section. Additionally, for nonvariational electron correlation methods, such as the four-component perturbation and coupled-cluster methods, the formulation procedure using a Lagrangian in the RISM-SCF method is now well established. For solvent models, more accurate models such as three-dimensional (3D) RISM[44,45] and the molecular Orenstein–Zernike (MOZ)[46,47] model that are compatible with the four-component relativistic method describing fine electronic structures of solutes, are desired. The 3D-RISM theory explicitly incorporates the orientation of one molecule in the two-body interaction between molecules, and the

1096987x, 2023, 1, Downloaded from https://onlinelibrary.wiley.com/doi/10.1002/jcc.27009 by Kyushu University, Wiley Online Library on [21/11/2022]. See the Terms and Conditions (https://onlinelibrary.wiley.com/terms-and-conditions) on Wiley Online Library for rules of use; OA articles are governed by the applicable Creative Commons License

MOZ theory explicitly incorporates the orientations of both molecules, resulting in the 3D-RISM-SCF[48,49] and MOZ-SCF[32,50] methods using these models to refine the description of solute–solvent intermolecular interactions. Those developments are currently in progress.

ACKNOWLEDGMENT

This work was supported by the Japan Society for the Promotion of Science (JSPS) Kakenhi (Grant Number: 21K04980 to Haruyuki Nakano, 19H02677 and 22H05089 to Norio Yoshida). Numerical calculations were partially cconducted at the Research Center for Computational Science, Institute for Molecular Science, National Institutes of Natural Sciences (Project: 22-IMS-C076) and using MCRP-S at the Center for Computational Sciences, University of Tsukuba.

DATA AVAILABILITY STATEMENT

The data that support the findings of this study are available from the corresponding authors upon reasonable request.

ORCID

Yoshihiro Watanabe https://orcid.org/0000-0001-9729-6810
Norio Yoshida https://orcid.org/0000-0002-2023-7254
Haruyuki Nakano https://orcid.org/0000-0002-7008-0312

REFERENCES

[1] W. Greiner, *Relativistic Quantum Mechanics. Wave Equations*, Springer, Berlin, Heidelberg **2000**.
[2] B. Bertha Swirles, *Proc. R. Soc. Lond. Ser. A: Math. Phys. Sci.* **1935**, *152*, 625.
[3] I. P. Grant, *Proc. R. Soc. Lond. Ser. A: Math. Phys. Sci.* **1961**, *262*, 555.
[4] G. Malli, J. Oreg, *J. Chem. Phys.* **1975**, *63*, 830.
[5] L. Visscher, O. Visser, P. J. C. Aerts, H. Merenga, W. C. Nieuwpoort, *Comput. Phys. Commun.* **1994**, *81*, 120.
[6] E. Engel, R. M. Dreizler, *Density Functional Theory II*, Springer-Verlag, Berlin/Heidelberg **1996**, p. 1.
[7] L. Belpassi, L. Storchi, H. M. Quiney, F. Tarantelli, *Phys. Chem. Chem. Phys.* **2011**, *13*, 12368.
[8] W. R. Johnson, M. Idrees, J. Sapirstein, *Phys. Rev. A* **1987**, *35*, 3218.
[9] Y. Ishikawa, *Phys. Rev. A* **1990**, *42*, 1142.
[10] K. G. Dyall, *Chem. Phys. Lett.* **1994**, *224*, 186.
[11] L. Visscher, T. Saue, W. C. Nieuwpoort, K. Faegri, O. Gropen, *J. Chem. Phys.* **1993**, *99*, 6704.
[12] Y. Watanabe, O. Matsuoka, *J. Chem. Phys.* **2002**, *116*, 9585.
[13] L. Visscher, T. J. Lee, K. G. Dyall, *J. Chem. Phys.* **1996**, *105*, 8769.
[14] O. Matsuoka, N. Suzuki, T. Aoyama, G. Malli, *J. Chem. Phys.* **1980**, *73*, 1320.
[15] H. J. A. Jensen, K. G. Dyall, T. Saue, K. Fægri, *J. Chem. Phys.* **1996**, *104*, 4083.
[16] T. Fleig, J. Olsen, L. Visscher, *J. Chem. Phys.* **2003**, *119*, 2963.
[17] Y. Ishikawa, M. J. Vilkas, K. Koc, *Int. J. Quantum Chem.* **2000**, *77*, 433.
[18] M. Miyajima, Y. Watanabe, H. Nakano, *J. Chem. Phys.* **2006**, *124*, 44101.
[19] M. Abe, T. Nakajima, K. Hirao, *J. Chem. Phys.* **2006**, *125*, 234110.
[20] T. Fleig, L. K. Sørensen, J. Olsen, *Theor. Chem. Accounts* **2007**, *118*, 347.
[21] R. J. Anderson, G. H. Booth, *J. Chem. Phys.* **2020**, *153*, 184103.
[22] S. Knecht, Ö. Legeza, M. Reiher, *J. Chem. Phys.* **2014**, *140*, 041101.
[23] R. Di Remigio, R. Bast, L. Frediani, T. Saue, *J. Phys. Chem. A* **2015**, *119*, 5061.
[24] E. Cancès, B. Mennucci, J. Tomasi, *J. Chem. Phys.* **1997**, *107*, 3032.
[25] R. D. R. D. Remigio, M. Repisky, S. Komorovsky, P. Hrobarik, L. Frediani, K. Ruud, *Mol. Phys.* **2017**, *115*, 214.
[26] E. D. Hedegård, R. Bast, J. Kongsted, J. M. H. Olsen, H. J. A. Jensen, *J. Chem. Theory Comput.* **2017**, *13*, 2870.
[27] D. Chandler, H. C. Andersen, *J. Chem. Phys.* **1930**, *1972*, 57.
[28] F. Hirata, in *Molecular Theory of Solvation*, Vol. 24 (Ed: F. Hirata), Kluwer Academic Publishers, Dordrecht **2004**.
[29] S. Ten-no, F. Hirata, S. Kato, *Chem. Phys. Lett.* **1993**, *214*, 391.
[30] S. Ten-no, F. Hirata, S. Kato, *J. Chem. Phys.* **1994**, *100*, 7443.
[31] H. Sato, F. Hirata, S. Kato, *J. Chem. Phys.* **1996**, *105*, 1546.
[32] N. Yoshida, Yoshida, *Condens. Matter Phys.* **2007**, *10*, 363.
[33] F. A. Momany, *J. Phys. Chem.* **1978**, *82*, 592.
[34] S. R. Cox, D. E. Williams, *J. Comput. Chem.* **1981**, *2*, 304.
[35] T. H. Dunning, *J. Chem. Phys.* **1989**, *90*, 1007.
[36] D. E. Woon, T. H. Dunning, *J. Chem. Phys.* **1993**, *98*, 1358.
[37] K. G. Dyall, *Theor. Chem. Accounts* **2006**, *115*, 441.
[38] A. K. Rappé, C. J. Casewit, K. S. Colwell, W. A. Goddard, W. M. Skiff, *J. Am. Chem. Soc.* **1992**, *114*, 10024.
[39] Y. Sakiyama, S. Takagi, Y. Matsumoto, *J. Chem. Phys.* **2005**, *122*, 234501.
[40] H. J. C. Berendsen, J. R. Grigera, T. P. Straatsma, *J. Phys. Chem.* **1987**, *91*, 6269.
[41] DIRAC a relativistic ab initio electronic structure program, Release DIRAC19; A. S. P. Gomes, T. Saue, L. Visscher, H. J. A. Jensen, R. Bast, I. A. Aucar, V. Bakken, K. G. Dyall, S. Dubilland, U. Ekstrom, E. Eliav, T. Enevoldsen, E. Fasshauer, T. Fleig, O. Fossgaard, L. Halbert, E. D. Hedegard, T. Helgaker, B. Helmich-Paris, J. Henriksson, M. Ilias, Ch. R. Jacob, S. Knecht, S. Komorovsky, O. Kullie, J. K. Laerdahl, C. V. Larsen, Y. S. Lee, H. S. Nataraj, M. K. Nayak, P. Norman, G. Olejiniczak, J. Olsen, J. M. H. Olsen, Y. C. Park, J. K. Pedersen, M. Pernpointner, R. Di Remigio, K. Ruud, P. Salek, B. Schimmelpfennig, B. Senjean, A. Shee, J. Sikkema, A. J. Thorvaldsen, J. Thyssen, J. van Stralen, M. L. Vidal, S. Villaume, O. Visser, T. Winther, S. Yamamoto, **2019**. http://dx.doi.org/10.5281/zenodo.3572669 , see also http://www.diracprogram.org.
[42] T. Saue, R. Bast, A. S. P. Gomes, H. J. A. Jensen, L. Visscher, I. A. Aucar, R. Di Remigio, K. G. Dyall, E. Eliav, E. Fasshauer, T. Fleig, L. Halbert, E. D. Hedegård, B. Helmich-Paris, M. Iliaš, C. R. Jacob, S. Knecht, J. K. Laerdahl, M. L. Vidal, M. K. Nayak, M. Olejniczak, J. M. H. Olsen, M. Pernpointner, B. Senjean, A. Shee, A. Sunaga, J. N. P. van Stralen, *J. Chem. Phys.* **2020**, *152*, 204104.
[43] N. Yoshida, F. Hirata, *J. Comput. Chem.* **2006**, *27*, 453.
[44] D. Beglov, B. Roux, *J. Phys. Chem. B* **1997**, *101*, 7821.
[45] A. Kovalenko, F. Hirata, *Chem. Phys. Lett.* **1998**, *290*, 237.
[46] L. Blum, *J. Chem. Phys.* **1973**, *58*, 3295.
[47] L. Blum, A. J. Torruella, *J. Chem. Phys.* **1972**, *56*, 303.
[48] A. Kovalenko, F. Hirata, *J. Chem. Phys.* **1999**, *110*, 10095.
[49] H. Sato, A. Kovalenko, F. Hirata, *J. Chem. Phys.* **2000**, *112*, 9463.
[50] N. Yoshida, S. Kato, *J. Chem. Phys.* **2000**, *113*, 4974.

How to cite this article: K. Kanemaru, Y. Watanabe, N. Yoshida, H. Nakano, *J. Comput. Chem.* **2023**, *44*(1), 5. https://doi.org/10.1002/jcc.27009

1096987x, 2023, 1, Downloaded from https://onlinelibrary.wiley.com/doi/10.1002/jcc.27009 by Kyushu University, Wiley Online Library on [21/11/2022]. See the Terms and Conditions (https://onlinelibrary.wiley.com/terms-and-conditions) on Wiley Online Library for rules of use; OA articles are governed by the applicable Creative Commons License